

# Optical-power-dependent photodesorption kinetics of graphene studied by conductance response

Yang-Yang Hsu,<sup>1</sup> Chi-Yuan Lin,<sup>1,2</sup> Yi-Chun Lai,<sup>2</sup> Kun-Rui Wu,<sup>1</sup> Kwai-Kong Ng,<sup>1</sup> Chen-Shiung Chang,<sup>2</sup> Gou Chung Chi,<sup>2</sup> Pei-Chen Yu,<sup>2</sup> and Forest Shih-Sen Chien<sup>1,\*</sup>

<sup>1</sup>Department of Applied Physics, Tunghai University, Taichung 40704, Taiwan

<sup>2</sup>Department of Photonics and Institute of Electro-Optical Engineering, National Chiao Tung University, Hsinchu 30010, Taiwan

\*fsschien@thu.edu.tw

**Abstract:** The photodesorption kinetics of graphene with various UV laser power is studied by conductance response. Analytical expressions of the power-dependent photodesorption kinetics of graphene in ambience are derived. The photodesorption time constant  $\tau_d$ , steady current, and magnitude of modulation current, can be expressed as functions of the adsorption time constant  $\tau_a$ , desorption cross section  $\sigma$ , and photon flux density. Under illumination the steady occupation ratio of adsorbed O<sub>2</sub> on graphene is equal to  $\tau_d/\tau_a$ . It is suggested that the photodesorption of O<sub>2</sub> on graphene is attributed the injection of photogenerated hot electrons and is restricted by the density of antibonding states of O<sub>2</sub>.

©2015 Optical Society of America

**OCIS codes:** (160.5335) Photosensitive materials; (160.4236) Nanomaterials; (240.6700) Surfaces; (000.1570) Chemistry.

---

## References and links

1. A. K. Geim, "Graphene: status and prospects," *Science* **324**(5934), 1530–1534 (2009).
2. F. Schedin, A. K. Geim, S. V. Morozov, E. W. Hill, P. Blake, M. I. Katsnelson, and K. S. Novoselov, "Detection of individual gas molecules adsorbed on graphene," *Nat. Mater.* **6**(9), 652–655 (2007).
3. Y. Dan, Y. Lu, N. J. Kybert, Z. Luo, and A. T. C. Johnson, "Intrinsic response of graphene vapor sensors," *Nano Lett.* **9**(4), 1472–1475 (2009).
4. N. Mohanty and V. Berry, "Graphene-based single-bacterium resolution biodevice and DNA transistor: interfacing graphene derivatives with nanoscale and microscale biocomponents," *Nano Lett.* **8**(12), 4469–4476 (2008).
5. S.-Z. Liang, G. Chen, A. R. Harutyunyan, M. W. Cole, and J. O. Sofo, "Analysis and optimization of carbon nanotubes and graphene sensors based on adsorption-desorption kinetics," *Appl. Phys. Lett.* **103**(23), 233108 (2013).
6. Y. Shi, W. Fang, K. Zhang, W. Zhang, and L. J. Li, "Photoelectrical response in single-layer graphene transistors," *Small* **5**(17), 2005–2011 (2009).
7. P. Sun, M. Zhu, K. Wang, M. Zhong, J. Wei, D. Wu, Y. Cheng, and H. Zhu, "Photoinduced molecular desorption from graphene films," *Appl. Phys. Lett.* **101**(5), 053107 (2012).
8. J. Lin, J. Zhong, J. R. Kyle, M. Penchev, M. Ozkan, and C. S. Ozkan, "Molecular absorption and photodesorption in pristine and functionalized large-area graphene layers," *Nanotechnology* **22**(35), 355701 (2011).
9. R. Franchy, "Surface and bulk photochemistry of solids," *Rep. Prog. Phys.* **61**(6), 691–753 (1998).
10. R. J. Chen, N. R. Franklin, J. Kong, J. Cao, T. W. Tomblor, Y. Zhang, and H. Dai, "Molecular photodesorption from single-walled carbon nanotubes," *Appl. Phys. Lett.* **79**(14), 2258–2260 (2001).
11. S. Kazaoui, N. Minami, H. Yamawaki, K. Aoki, H. Kataura, and Y. Achiba, "Pressure dependence of the optical absorption spectra of single-walled carbon nanotubes films," *Phys. Rev. B* **62**(3), 1643–1646 (2000).
12. K. F. Mak, J. Shan, and T. F. Heinz, "Seeing many-body effects in single- and few-layer graphene: observation of two-dimensional saddle-point excitons," *Phys. Rev. Lett.* **106**(4), 046401 (2011).
13. D.-H. Chae, T. Utikal, S. Weisenburger, H. Giessen, K. V. Klitzing, M. Lippitz, and J. Smet, "Excitonic Fano resonance in free-standing graphene," *Nano Lett.* **11**(3), 1379–1382 (2011).
14. A. Das, S. Pisana, B. Chakraborty, S. Piscanec, S. K. Saha, U. V. Waghmare, K. S. Novoselov, H. R. Krishnamurthy, A. K. Geim, A. C. Ferrari, and A. K. Sood, "Monitoring dopants by Raman scattering in an electrochemically top-gated graphene transistor," *Nat. Nanotechnol.* **3**(4), 210–215 (2008).

15. L. W. Bruch, M. W. Cole, and E. Zaremba, *Physical Adsorption: Forces and Phenomena* (Dover Publications, New York, 2007).
16. P. D. Cooper, R. E. Johnson, and T. I. Quickenden, "A review of possible optical absorption features of oxygen molecules in the icy surfaces of outer solar system bodies," *Planet. Space Sci.* **51**(3), 183–192 (2003).
17. P. R. Antoniewicz, "Model for electron- and photon-stimulated desorption," *Phys. Rev. B* **21**(9), 3811–3815 (1980).
18. R. E. Palmer and P. J. Rous, "Resonances in electron scattering by molecules on surfaces," *Rev. Mod. Phys.* **64**(2), 383–440 (1992).
19. J. W. Gadzuk, "Excitation mechanisms in vibrational spectroscopy of molecules on surfaces," in *Vibrational Spectroscopy of Molecules on Surfaces*, J. T. Yates, Jr., and T. E. Madey, ed. (Springer, New York, 1987).
20. K. K. Irikura, "Experimental vibrational zero-point energies: diatomic molecules," *J. Phys. Chem. Ref. Data* **36**(2), 389–397 (2007).
21. P. Giannozzi, R. Car, and G. Scoles, "Oxygen adsorption on graphite and nanotubes," *J. Chem. Phys.* **118**(3), 1003–1006 (2003).

## 1. Introduction

Graphene [1], few atomic carbon layers in a honeycomb lattice, is the ultimate two-dimensional surface material without bulk effect. Because of its extremely high specific surface area and sensitive electrical response to molecular adsorption, graphene is regarded as an excellent candidate for chemical sensors [2–4]. The stable graphene-based sensors can sustain a great number of adsorption/desorption cycles. Typically, the gas molecules are physisorbed (weakly bound) on graphene and become the electron donors or acceptors to graphene. The carrier density of graphene is correlated to the density of adsorbed molecules, so adsorption results in the change of carrier density. It is assumed that the number of electron transferred per adsorbed molecule is constant and the adsorbates do not affect the charge mobility of graphene [5]. Hence the conductance change is proportional to the area density of adsorbates on graphene. Therefore the conductance response of graphene can be utilized to monitor the molecular adsorption and desorption, making graphene an ideal system to study the kinetics of adsorption and desorption.

The conductance response of graphene on photodesorption has been studied recently [5–8]. Photodesorption is a photophysical/photochemical process to efficiently achieve surface treatments [9]. The density of adsorbates on surface can be controlled by photodesorption. The conductance response of graphene on photodesorption follows the exponential function  $e^{-t/\tau_d}$  of exposure time  $t$ , where  $\tau_d$  is the photodesorption time constant. In ambience,  $O_2$  molecules act as electron acceptors for graphene and are the dominant species of adsorbates that influences the conductivity of graphene. Therefore, the density of adsorbed  $O_2$  on graphene  $N(t)$  under UV illumination in vacuum (without re-adsorption) is well described by the differential equation

$$\frac{dN(t)}{dt} = -\sigma FN(t), \quad (1)$$

where  $F$  is the photon flux density,  $\sigma$  the cross section of photodesorption, and  $\tau_d = \sigma^{-1}F^{-1}$  [10]. The photodesorption kinetics of adsorbates on graphene is of great scientific interest and is significant to the gas sensor applications. However, the optical power-dependent kinetics has not been illustrated clearly.

Furthermore, it has been reported that  $\sigma$  of single-walled carbon nanotubes (CNT) is strongly dependent on photon energy ( $E_{ph}$ ), such that  $\sigma$  increases by several orders of magnitude with photon energy ranged from near-infrared to UV [10]. It is suggested that such a photon-energy dependence of  $\sigma$  is attributed to the optical absorption of CNT (with an absorption peak at 5 eV) [11]. Graphene exhibits an absorption peak (at 4.7 eV) similar to that of CNT [12,13]. This optical absorption behavior of graphene is due to the excitonic Fano resonance arising from the coupling between the interband transition at the saddle point and the transition at the continuous Dirac cone. The  $E_{ph}$  dependence of  $\sigma$  in graphene is important to the understanding of the photodesorption mechanism of graphene, but is not well studied.

In this paper, we studied the UV-power-dependent photodesorption kinetics of graphene in ambience by monitoring the response current of graphene. An analytical expression of  $N(t)$  is derived to describe the power-dependent photodesorption kinetics (involving re-adsorption). From the expression of  $N(t)$ , the photodesorption quantities of current response (photodesorption time constant, steady current and magnitude of modulation current) can be expressed as functions of  $\tau_a$ ,  $\sigma$ , and  $F$ . Furthermore, the steady occupation ratio of photodesorption  $N_s/N_{\max} = \tau_d/\tau_a$  is obtained, where  $\tau_a$  is the adsorption time constant of graphene,  $N_s$  the steady density of  $O_2$ , and  $N_{\max}$  the maximum density of  $O_2$ . In addition, in order to investigate the underlying mechanism, the photodesorption is performed by the lasers of various  $E_{\text{ph}}$ . From the dependence of  $\sigma$  on  $E_{\text{ph}}$ , it is suggested that the photodesorption of graphene involves the injection of photogenerated hot electrons and is restricted by the density of antibonding states of  $O_2$ .

## 2. Experimental details

The graphene sample is grown on Cu foil by chemical vapor deposition (CVD). The CVD graphene is then transferred to  $\text{SiO}_2/\text{Si}$  substrate after the Cu foil is etched by  $\text{Fe}(\text{NO}_3)_3$  solution. Silver paste is used to make electrodes on the sample. A bias of 10 mV is applied for current measurement. The graphene is placed in an air-tight chamber to keep the relative humidity constant (40%) at room temperature. A 325 nm UV He-Cd laser is employed in the power-dependent desorption and solid state lasers of 405, 473, and 532 nm are employed in the  $E_{\text{ph}}$ -dependent photodesorption.

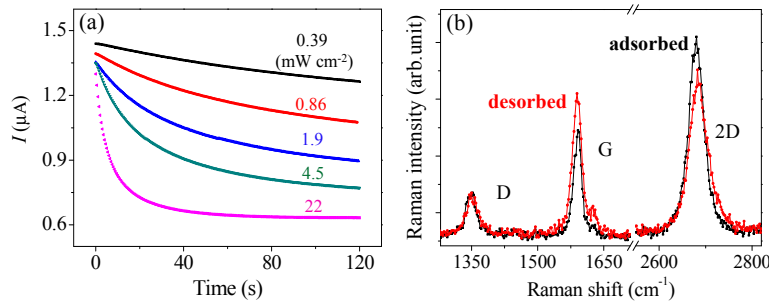


Fig. 1. (a) Response current of graphene on photodesorption with various UV power densities, and (b) Raman spectra of adsorbed and desorbed graphenes.

## 3. Results and discussion

### 3.1 Optical-power-dependent current response

The current response of graphene on photodesorption subjected to various power density level of UV laser (from 0.39  $\text{mW}/\text{cm}^2$  to 22  $\text{mW}/\text{cm}^2$ ) is observed as shown in Fig. 1(a). The currents decrease exponentially from the initial current ( $I_0$ ), because the hole density decreases with the photodesorption of  $O_2$ . The Raman spectra of adsorbed and desorbed graphenes are presented in Fig. 1(b). The intensity ratio of the G peak to 2D peak indicates that the sample is a monolayer or bilayer graphene. The D peak indicates the existence of defects in the CVD graphene. In desorption, a red shift of G band and a blue shift of 2D band suggest the hole de-doping occurs in the graphene [14].

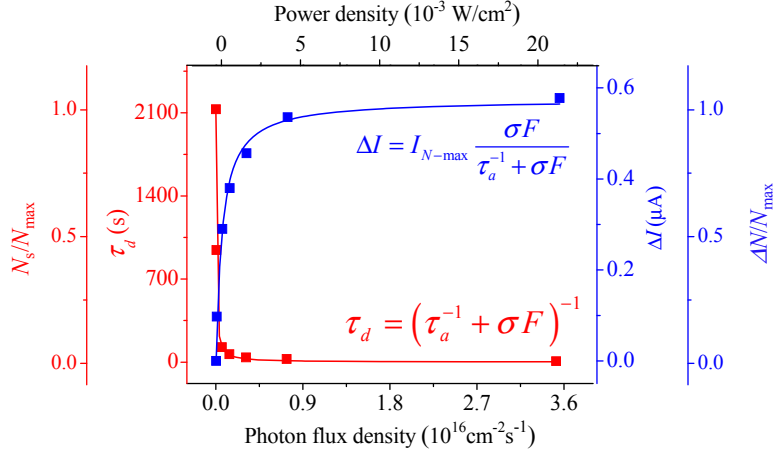


Fig. 2. Photodesorption time constant  $\tau_d$  (as well as  $N_s/N_{\max}$  referring to the second ordinate on the left hand side) and  $\Delta I$  (as well as  $\Delta N/N_{\max}$  referring to the second ordinate on the right side) as functions of the photon flux density (and power density). The solid line are the fittings from Eqs. (7) and (8).

The response current can be described by a function of time  $t$  as

$$I(t) = I_s + \Delta I \cdot e^{-t/\tau_d}, \quad (2)$$

where  $I_s$  is the steady current at  $t = \infty$ , and  $\Delta I = I_0 - I_s$  is the magnitude of current modulation due to photodesorption. The optical-power-dependent response current on photodesorption can be well fitted with Eq. (2), and the  $F$  dependence of  $\tau_d$  and  $\Delta I$  are obtained (1 mW/cm<sup>2</sup> of 325 nm corresponds to the photon flux density of  $1.64 \times 10^{15}$  cm<sup>-2</sup> s<sup>-1</sup>) (Fig. 2). In addition,  $I_s$  and  $\Delta I$  are plotted as functions of  $\tau_d$  (Fig. 3).  $I_s$  and  $\Delta I$  show a positive and negative linear relationship with  $\tau_d < 75$  s, respectively. When the laser is switched off, O<sub>2</sub> molecules start to re-adsorb on graphene. Accordingly, the current increases in another exponential form with the adsorption time constant  $\tau_a$ , and is expressed as

$$I(t) = I_0 - \Delta I \cdot e^{-t/\tau_a}, \quad (3)$$

where  $\tau_a$  is about 2130 s and  $I(\infty) = I_0$ .

### 3.2 Kinetics of photodesorption

It is natural to assume that the current attributed to the density of adsorbed O<sub>2</sub> is given as  $I_N(t) = kN(t)$ , where  $k$  is a constant coefficient. From Eq. (3), we propose the adsorption differential equation of the O<sub>2</sub> density on graphene as

$$\frac{dN(t)}{dt} = \tau_a^{-1}(N_{\max} - N(t)). \quad (4)$$

If the laser is turned off at  $t = 0$ , and we let  $N(0) = N_s$  and  $N(\infty) = N_{\max}$ . The current associated with  $N_{\max}$  is  $I_{N-\max} = kN_{\max}$  and  $\Delta I = k(N_{\max} - N_s)$ . Besides the charge density induced O<sub>2</sub>, there is an intrinsic charge density in graphene that contributes an intrinsic current  $I_i$ . The currents are thus  $I(t) = I_N(t) + I_i$ ,  $I_0 = I_{N-\max} + I_i$ , and  $I_s = kN_s + I_i$ .

To understand the kinetics of photodesorption on graphene, the differential equation for photodesorption in ambience (modified from the Langmuir model [15]) is proposed as

$$\frac{dN(t)}{dt} = \tau_a^{-1}(N_{\max} - N(t)) - \sigma FN(t). \quad (5)$$

Solving the differential equation with the boundary conditions,  $N(0) = N_{\max}$  and  $N(\infty) = N_s$ , gives the adsorbate density as

$$N(t) = N_{\max} \left( \frac{\tau_a^{-1}}{\tau_a^{-1} + \sigma F} \right) + N_{\max} \left( \frac{\sigma F}{\tau_a^{-1} + \sigma F} \right) e^{-(\tau_a^{-1} + \sigma F)t}, \quad (6)$$

and  $N_s = N_{\max} [\tau_a^{-1} / (\tau_a^{-1} + \sigma F)]$  and  $\Delta N = N_{\max} - N_s = N_{\max} [\sigma F / (\tau_a^{-1} + \sigma F)]$ . By comparing Eqs. (2) and (6), the analytical expressions of  $\tau_d$ ,  $\Delta I$  and  $I_s$  as functions of  $F$  are derived as

$$\tau_d = (\tau_a^{-1} + \sigma F)^{-1}, \quad (7)$$

$$\Delta I = I_{N-\max} \frac{\sigma F}{\tau_a^{-1} + \sigma F}, \text{ and} \quad (8)$$

$$I_s = I_{N-\max} \frac{\tau_a^{-1}}{\tau_a^{-1} + \sigma F} + I_i. \quad (9)$$

$\Delta I$  and  $I_s$  in Eqs. (8) and (9) can also be rewritten as linear functions of  $\tau_d$ , as

$$\Delta I = I_{N-\max} \left( 1 - \frac{\tau_d}{\tau_a} \right), \text{ and} \quad (10)$$

$$I_s = I_{N-\max} \frac{\tau_d}{\tau_a} + I_i, \quad (11)$$

where  $\Delta I$  and  $I_s - I_i$  are complementary. The dependence of  $\tau_d$  and  $\Delta I$  on  $F$  in Fig. 2 is well fitted by Eqs. (7) and (8), indicating the validity of those expressions derived from the photodesorption kinetics of Eq. (6). Fitting the plot of  $\tau_d$  vs.  $F$  with Eq. (7), we obtain the cross section  $\sigma = 6 \times 10^{-18} \text{ cm}^2$  under UV laser illumination, which is similar to the reported value of CNT ( $1.4 \times 10^{-17} \text{ cm}^2$ ) by 254 nm UV [10]. It is noted that the contribution of re-adsorption cannot be ignored when  $\tau_a$  is small or  $F$  is low; otherwise  $\sigma$  will be overestimated.

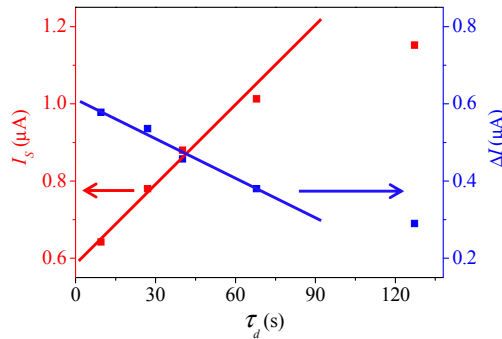


Fig. 3. Dependence of  $I_s$  and  $\Delta I$  on  $\tau_d$ .

Equations (10) and (11) account for the linear relationship of  $I_s$  and  $\Delta I$  with  $\tau_d$  in Fig. 3.  $I_s$  and  $\Delta I$  deviates from the linear relation when  $\tau_d$  is large (i.e., low  $F$ ), because the measuring time (120 s) is much shorter than  $\tau_d$  in Fig. 1(a) and a significant uncertainty occurs to the fitted  $I_s$  and  $\Delta I$ . According to Eq. (11), the intersection of the fitted line of  $I_s$  with the vertical axis shows  $I_i \cong 0.6 \text{ } \mu\text{A}$  in our case. Based on the above arguments, the photodesorption

quantities ( $\tau_d$ ,  $\Delta I$  and  $I_s$ ) of response current of graphene can be well described by the analytical expressions [Eqs. (7)-(11)]. For  $t = \infty$ , the steady occupation ratio  $N_s/N_{\max}$  and unoccupation ratio  $\Delta N/N_{\max}$  on graphene can be given directly from measured currents,

$$\frac{N_s}{N_{\max}} = \frac{I_s - I_i}{I_0 - I_i}, \text{ and } \frac{\Delta N}{N_{\max}} = \frac{\Delta I}{I_0 - I_i}. \quad (12)$$

Interestingly, these steady ratios can also be derived from from Eq. (6) in terms of the characteristic time constants:

$$\frac{N_s}{N_{\max}} = \frac{\tau_d}{\tau_a}, \text{ and } \frac{\Delta N}{N_{\max}} = 1 - \frac{\tau_d}{\tau_a}. \quad (13)$$

Therefore, the  $F$  dependence of  $N_s/N_{\max}$  and  $\Delta N/N_{\max}$  can be translated from either the  $F$  dependence of  $I_s$  and  $\Delta I$  in Eqs. (8) and (9) or the  $F$  dependence of  $\tau_d$  in Eq. (7). For examples,  $N_s/N_{\max}$  is derived from  $\tau_d$ , and  $\Delta N/N_{\max}$  from  $\Delta I$ , respectively, as illustrated in Fig. 2. Thus Eqs. (12) and (13) are very useful to estimate the steady occupation and unoccupation ratios of photodesorption.

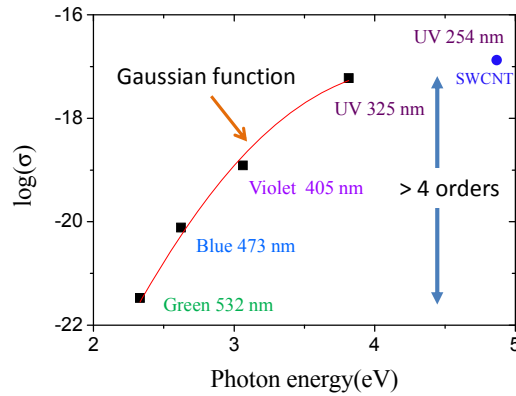


Fig. 4. Dependence of cross section  $\sigma$  of graphene on photon energy, including the cross section  $\sigma$  of single-walled CNTs by 254 nm UV light [10].

### 3.3 $E_{\text{ph}}$ -dependent photodesorption

To explore the photodesorption mechanism of graphene, we investigate the dependence of  $\sigma$  on  $E_{\text{ph}}$ . Lasers of different wavelengths (325 nm, 405 nm, 473 nm and 532 nm) are applied to obtain the  $E_{\text{ph}}$ -dependent  $\sigma$  by Eq. (7), as shown in Fig. 4.  $\sigma$  increases by more than four orders of magnitude with  $E_{\text{ph}}$  ranged from 2.33 eV to 3.82 eV. However, the optical absorbance of graphene increases only from 2.3% (off resonance) to 11% (at resonance) [13]. Such a small absorbance change with  $E_{\text{ph}}$  cannot account for the dramatic change in  $\sigma$ . There are two types of possible mechanisms responsible for the photodesorption: the adsorbate excitation and substrate excitation [10]. Because the electronic transition from the fundamental state ( $X^3\Sigma_g^-$ ) to the excited state ( $A^3\Sigma_u^+$ ) of  $O_2$  occurs at wavelengths  $< 270$  nm, known as the Herzberg continuum (i.e.,  $O_2$  is transparent to visible light) [16], the adsorbate ( $O_2$ ) excitation does not account for the desorption from visible to UV we observe here. Therefore the substrate (graphene) excitation is the only possible underlying mechanism for the photodesorption of  $O_2$ .

The incident photons are absorbed by graphene to excite the electronic interband ( $\pi$  orbital to  $\pi^*$  orbital) transition. There are two possible paths for the excited electrons to induce

photodesorption: photothermal reaction and hot electron injection. Photodesorption can occur even the power density is as low as  $0.14 \text{ mW/cm}^2$ , which is, however, too low to raise the temperature of substrate and graphene. Hence the photodesorption of graphene is not a photothermal reaction. We suggest that the photodesorption is evoked by the photogenerated hot electrons in graphene (Fig. 5(a)) [17,18]. By tunneling, the hot electrons transit into the antibonding orbital of  $\text{O}_2$  to form excited negative oxygen ions. The short-lived negative ions at the ground vibronic level relax into neutral molecules at the excited vibronic level by another electron tunneling (to graphene) via the Franck-Condon transition (Fig. 5(b)) [19]. The excited vibronic state of  $\text{O}_2$  has the vibrational zero-point energy with harmonic frequency  $\approx 1580 \text{ cm}^{-1}$  [20], which exceeds the binding energy of  $\text{O}_2$  on graphene ( $\sim 100 \text{ meV}$ ) [21] and causes the desorption of  $\text{O}_2$ . Assume that  $\sigma(E_{\text{ph}})$  is proportional to  $\alpha_{\text{abs}}(E_{\text{ph}}) \cdot \eta_t(E_{\text{ph}}) \cdot \rho_{\text{oxy}}(E_{\text{ph}})$ , where  $\alpha_{\text{abs}}(E_{\text{ph}})$  is the optical absorbance of graphene,  $\eta_t(E_{\text{ph}})$  the hot electron tunneling rate between graphene and  $\text{O}_2$ , and  $\rho_{\text{oxy}}(E_{\text{ph}})$  the density of antibonding states of  $\text{O}_2$ . From  $E_{\text{ph}} = 2.33 \text{ eV}$  to  $3.82 \text{ eV}$ ,  $\alpha_{\text{abs}}(E_{\text{ph}})$  increases by a factor of 2 [13] and  $\eta_t(E_{\text{ph}})$  by a factor of 1.46 [estimated by the transmittance of tunneling, having the square potential barrier height =  $5 \text{ eV}$  (the work function of graphene), and width =  $4 \text{ \AA}$  (the size of  $\text{O}_2$ )]. Thus  $\rho_{\text{oxy}}(E_{\text{ph}})$  is the remaining dominant term of the photodesorption of  $\text{O}_2$ , responsible for a factor of  $10^4$  of the change in  $\sigma(E_{\text{ph}})$ , because  $\rho_{\text{oxy}}(E_{\text{ph}})$  decreases rapidly as the electron energy is away from the band center of the antibonding orbital of  $\text{O}_2$ .

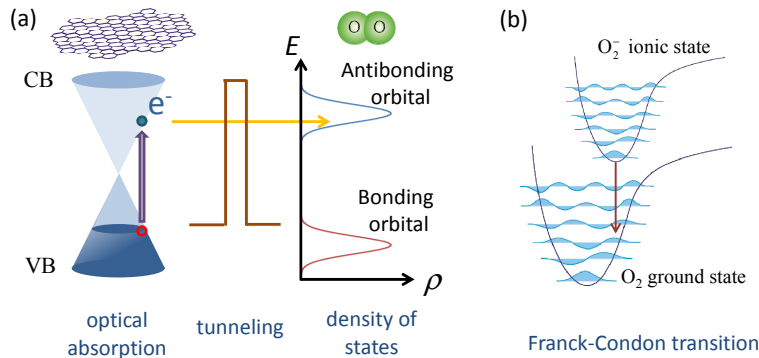


Fig. 5. (a) Photodesorption mechanism of graphene: (from left to right) excitation of electrons by the optical absorption of graphene, electron tunneling from graphene to the antibonding orbital of  $\text{O}_2$ , and  $\text{O}_2$  acquires kinetic energy to desorb via the Franck-Condon transition. (b) Schematic of the vibronic levels of  $\text{O}_2$  and  $\text{O}_2^-$  to illustrate the Franck-Condon transition.

#### 4. Conclusion

The UV-laser photodesorption of CVD graphene in air is studied by the current response. The analytical expressions of the power-dependent photodesorption kinetics are derived to describe the current response of graphene under illumination. The photodesorption quantities of current response ( $\tau_d$ ,  $I_s$  and  $\Delta I$ ) can be expressed as functions of  $\tau_a$ ,  $\sigma$ , and  $F$ . Additionally, the steady occupation rate of  $\text{O}_2$  on graphene  $N_s/N_{\text{max}} = \tau_d/\tau_a$  is derived. The photodesorption cross section  $\sigma$  of graphene increases by four orders of magnitude as  $E_{\text{ph}}$  increases from  $2.33 \text{ eV}$  to  $3.82 \text{ eV}$ . It is suggested that the photodesorption of adsorbed  $\text{O}_2$  on graphene is induced by the photogenerated hot electrons and is restricted by the density of antibonding states of  $\text{O}_2$ .

#### Acknowledgments

This work was supported by the Ministry of Science and Technology of Taiwan (Grant No. MOST 102-2112-M-029-005-MY3).